

# Gaze-guided Hand-Object Interaction Synthesis: Benchmark and Method

Jie Tian, Lingxiao Yang, Ran Ji, Yuexin Ma, Lan Xu, Jingyi Yu, Ye Shi, and  
Jingya Wang

ShanghaiTech University

**Abstract.** Gaze plays a crucial role in revealing human attention and intention, shedding light on the cognitive processes behind human actions. The integration of gaze guidance with the dynamics of hand-object interactions boosts the accuracy of human motion prediction. However, the lack of datasets that capture the intricate relationship and consistency among gaze, hand, and object movements remains a substantial hurdle. In this paper, we introduce the first Gaze-guided Hand-Object Interaction dataset, GazeHOI, and present a novel task for synthesizing gaze-guided hand-object interactions. Our dataset, GazeHOI, features simultaneous 3D modeling of gaze, hand, and object interactions, comprising 479 sequences with an average duration of 19.1 seconds, 812 sub-sequences, and 33 objects of various sizes. We propose a hierarchical framework centered on a gaze-guided hand-object interaction diffusion model, named GHO-Diffusion. In the pre-diffusion phase, we separate gaze conditions into spatial-temporal features and goal pose conditions at different levels of information granularity. During the diffusion phase, two gaze-conditioned diffusion models are stacked to simplify the complex synthesis of hand-object motions. Here, the object motion diffusion model generates sequences of object motions based on gaze conditions, while the hand motion diffusion model produces hand motions based on the generated object motion. To improve fine-grained goal pose alignment, we introduce a Spherical Gaussian constraint to guide the denoising step. In the subsequent post-diffusion phase, we optimize the generated hand motions using contact consistency. Our extensive experiments highlight the uniqueness of our dataset and the effectiveness of our approach.

## 1 Introduction

Gaze serves as a significant behavioral signal, rich with information on intent. In the field of visual cognition, researchers extensively explore the relationship between gaze, attention, and human activities. [15,43] note that the gaze system is pivotal in understanding how humans perceive the environment and gather information. Therefore, understanding the distribution of gaze at the level of spatial and temporal is fundamental to understanding any visually driven behavior. Different tasks elicit varying gaze behaviors, yet there is a consistency across individuals. This consistency provides theoretical support for our exploration

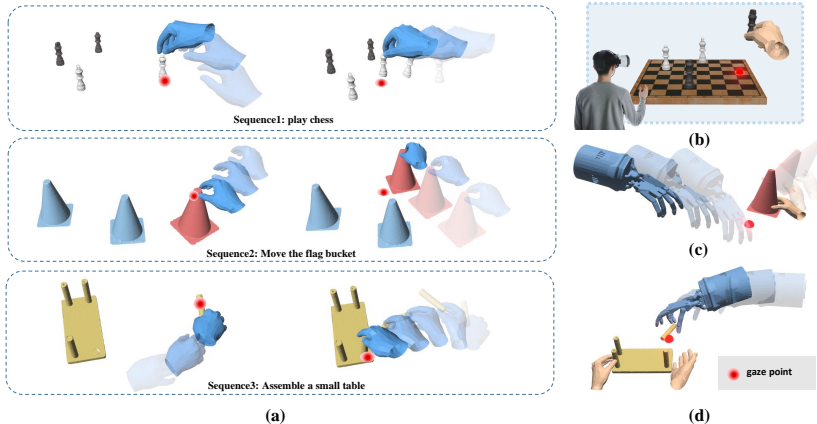


**Fig. 1:** The gazes contain abundant information represented as red dots, implying what object people want to manipulate and where to place them. (a) shows 3 sequences in GazeHOI, which illustrate gaze information can play a guidance role in hand-object interaction in daily life, such as playing chess, moving buckets, and assembling a small table. The other parts illustrate the future applications with possibilities, (b) depict using gaze to play VR chess, (c) demonstrate obstacle avoidance in human-robot interaction, and (d) showcases silky-smooth collaboration achieved through gaze interaction with the robot.

of the information embedded between gaze and the spatial-temporal variations of human motions. Besides, [8] highlights the close relationship between gaze and grasping poses. Based on this, we believe that examining the consistent relationships among gaze, hand, and object can enhance our understanding of human activities in fine-grained scenarios and the logic of interaction between humans and objects. This, in turn, can benefit and be applied to virtual reality (VR), augmented reality (AR), and human-robot interaction (HRI) contexts. As illustrated in Figure 1(b), VR users can control a game of chess through gaze, and future integration with technologies such as EEG could enhance the fluidity of playing chess in VR environments. In HRI scenarios, exploring the information within the human gaze can help eliminate ambiguities in movement, thereby empowering robots with a deeper comprehension of human activities. By forecasting actions that could potentially lead to dangerous situations and preemptively formulating solutions, this approach realizes more secure interactions as depicted in Figure 1(c). Moreover, this methodology paves the way for a novel paradigm in human-robot collaboration that doesn't rely on explicit command signals. Instead, robots are equipped to interpret and respond to subtle cues from the human gaze. An illustrative example of this, shown in Figure 1(d), involves a robotic arm intuitively recognizing a person's intent to pick up a table leg, thereby assisting in the table assembly by handing over the necessary parts.

Previous work [1, 11, 13, 16, 22, 31] primarily focused on extracting intent from gaze without delving deeper to extract more comprehensive information. [23, 63] have bridged the gap from gaze to intent and further to motion, enabling the extraction of motion information directly from gaze data. However, these stud-

ies largely concentrated on the broad movements of individuals within scenes, lacking exploration into the hand and detailed interactions within fine-grained environments. Consequently, we introduce a novel task: gaze-guided hand-object interaction synthesis. Addressing this task presents us with three significant challenges: **First**, there is a lack of suitable datasets. Current datasets on hand-object interactions focus solely on the interactions between hands and objects, overlooking the corresponding gaze during these interactions. Moreover, datasets that do include gaze data often lack 3D modeling of the hands and objects. **Second**, the challenge lies in how to extract the motion priors that can guide interaction synthesis. While GIMO [63] provides an excellent approach for capturing spatiotemporal information from gaze, it primarily focuses on activities within static scenes and lacks interaction modeling. **Third**, synthesizing both hands and objects necessitates a higher standard for movement consistency. The common approach is to deconstruct the task into different stages, to ensure consistency across each stage of the process, which, in turn, places new demands on precise and controllable generation.

In response to the challenges outlined above, we have devised specific solutions. Firstly, we collect the first interaction dataset that simultaneously incorporates 3D modeling of gaze, hand, and object interactions, thereby addressing a notable void in the research field. To address the second challenge, We decoupled the gaze-guided conditions into spatial-temporal feature encoding and goal pose generation using the gaze-contact consistency value to extract features in different levels of information granularity. In response to the third challenge, we propose a hierarchical framework centered on GHO-Diffusion and introduce the Spherical Gaussian constraint in the diffusion denoising step for precise and natural guidance and leverage contact consistency in the post-diffusion phase.

Our contributions can be summarized as follows:

1. **Introduction of the GazeHOI Dataset:** This is the first dataset specifically designed to explore gaze-guided hand-object interactions. It comprises 479 sequences, 812 subsequences, and 33 objects of varying sizes, providing a comprehensive resource for studying the complex interaction between human hands, objects, and gaze.
2. **Development of the GHO-Diffusion Model:** The paper presents a novel hierarchical framework centered on the GHO-Diffusion model for synthesizing gaze-guided hand-object interactions. This model innovatively separates gaze conditions into spatial-temporal features and goal pose conditions, employing two stacked gaze-conditioned diffusion models to simplify the synthesis of complex hand-object motions.
3. **Innovative Techniques for Hand-Object Motion Synthesis:** By introducing the Spherical Gaussian constraint in the diffusion denoising step and leveraging contact consistency in the post-diffusion phase, this work proposes new methods to improve fine-grained goal pose alignment and optimize generated hand motions. These techniques contribute to enhancing the accuracy and realism of gazed-guided hand-object interaction synthesis.

## 2 Related Work

***Predicting and Utilizing Gaze for Perception.*** Gaze serves as a crucial behavioral signal, encapsulating a wealth of intentional cues. It provides insights into individuals’ attention, interest, and cognitive processes, making it a fundamental aspect of human interaction and communication. Due to the expense and accuracy limitations of gaze tracking equipment, the previous researchers have primarily explored methods for estimating gaze from a third-person perspective images or videos [1, 13, 16, 22]. With the recent advancements in gaze tracking technology, acquiring accurate gaze information has become relatively more convenient, leading to the emergence of numerous datasets [7, 11, 23, 40, 63] containing gaze annotations. Researchers have moved beyond solely acquiring gaze data and are now exploring methods for extracting rich information inherent in gaze signals. [11] applies gaze to the field of autonomous driving, inferring the ego-trajectory of a driver’s vehicle. [31] explore predicting interaction intentions through gaze in human-object interaction scenarios, while limiting to predict action labels. [23, 63] propose leveraging gaze to predict human motions within the scene, which reveals the potential of gaze in virtual reality (VR) and human-robot interaction scenarios. However, they solely focus on human motions, overlooking the finer granularity of the hands, which play a pivotal role in human interaction with the environment. Therefore, in this work, we introduce the task of gaze-guided hand-object interaction motion synthesis and collect the first dataset containing synchronized hand, object, and gaze information for hand-object interaction.

***Hand-Object Interaction Dataset.*** Numerous datasets [4, 12, 17, 25, 33, 34, 56, 58, 61] dedicated to hand-object interactions have been developed to facilitate the capture of hand and object poses and to deepen our understanding of these interactions, as shown in Table 1. While many datasets [12, 17, 25, 56] feature scenes with only a single object, diverging from real-world settings where hand-object interactions often involve multiple objects of varying sizes, necessitating more complex operations and refined annotations. DexYCB [4] places multiple objects on a table during collection but interacts with only one object at a time. In HOI4D [34], scenarios involving simultaneous interactions with multiple objects, such as pouring water, are included. However, HOI4D solely utilizes an egocentric viewpoint for data collection, which leaves room for improvement in terms of data accuracy. TACO [33] captures scenes of simultaneous interactions with multiple objects, yet it lacks extended continuous interactions. Furthermore, these datasets, during their collection, focus solely on the relationship between hands and objects, overlooking the role of gaze. Therefore, we introduce a comprehensive dataset from an egocentric perspective, enriched with detailed gaze annotations and complex tasks, which we define as serialized motions involving continuous interactions with multiple objects. It captures the dynamics of hand-object interactions across a wide range of tasks from the arrangement of chess pieces to the assembly of furniture. We aim to bridge the gap in current datasets by offering a resource that mirrors the multifaceted nature of real-world

	Gaze	Ego	Multi-obj	Complex-Task	#views	#images
HO-3D [17]	×	×	×	×	1-4	78K
DexYCB [4]	×	×	×	×	8	508K
H2O [25]	×	✓	×	×	5	685K
OakInk [56]	×	×	×	×	4	230K
HOI4D [34]	×	✓	×	×	2	2.4M
ARCTIC [12]	×	✓	×	×	9	2.1M
TACO [33]	×	✓	✓	×	13	5.2M
GazeHOI	✓	✓	✓	✓	13	3.2M

**Table 1:** Comparison of GazeHOI with existing 4D hand-object interaction datasets. interactions, highlighting the significance of gaze in predicting human intent and the complexity of multi-object manipulation.

**Hand-Object Motion Synthesis.** Recently, considerable attention has been directed towards the advancement of human-object motion synthesis methods, prominently using Conditional Variational AutoEncoder(cVAE) [14,28,48,52] or Diffusion models [21,24,29,30,38,49–51,54,60]. However, a notable gap persists in the synthesis process, particularly concerning the reconstruction of hand motion during object interaction, for most work neglects the fine-grained reconstruction of the hand motion, or only generates the motion sequence up to the grasping pose, thus failing to capture continuous interaction between the hand and the object. In the field of hand-object motion synthesis, prior efforts have mainly centered on frame-wise generation [20,26]. While some endeavors have realized the generation of motion sequence [3,5,57,62], they often rely on some explicit conditions such as given object pose [57,62] or grasp reference [5]. As for conditions of motion synthesis, many existing methods utilize various modalities, including text cues [50], initial or final human pose [14,48], object geometry [20,26], contact map [26], trajectory [21,57], etc., while the gaze condition is often overlooked. In this work, our primary emphasis lies on the integration of the gaze condition as a foundational element in the synthesis of realistic hand-object motion and considers the process of continuous interaction between hands and objects.

### 3 Dataset

Currently, available datasets Table 1 mainly focus on the interaction relationship between hand-objects, ignoring the role of GAZE, a complete interaction requires coordinated hand-eye-object cooperation. We therefore propose the first interaction dataset that simultaneously includes gaze-hand-object 3D modeling, filling a gap in the field. The GazeHOI dataset covers a wide range of interaction complexity, from basic one-handed tasks to complex two-handed furniture assembly operations that require two-handed cooperation. In addition, our dataset aligns well with images and can also support hand-object interaction reconstruction tasks. The details of the data collecting system and baselines about hand-object interaction reconstruction will be shown in the supplementary.

#### 3.1 Data Collection

We recruited 10 volunteers (5 males and 5 females) to assist us in data collection. Before the collection process, we provided the participants with a comprehensive script (available in the supplementary) that detailed the tasks they were

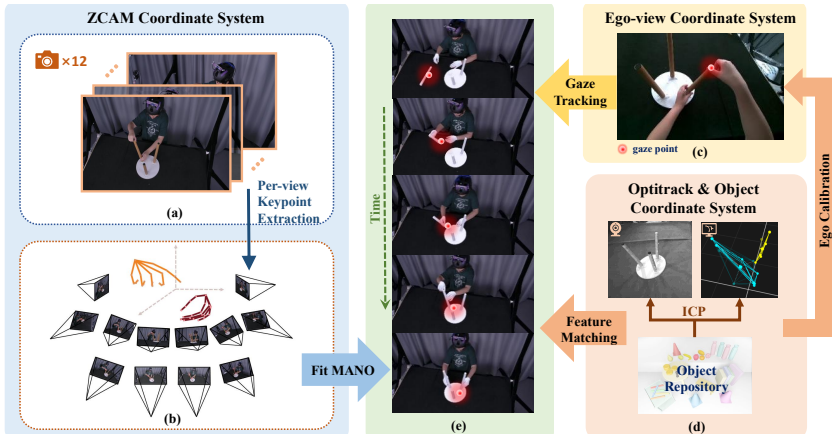


**Fig. 2:** Automatic data processing pipeline. (a) displays 12-view images from the raw video. (b) uses mediapipe [35] to get hand 2d keypoints and triangulation to obtain the 3d keypoints. (c) shows the ego view with a gaze point. (d) illustrates the 37 objects acquired by the scanner and the marker tracking process. (e) shows the result of human-object motion synthesis.

required to complete. For each task, participants were asked to perform multiple iterations. Consequently, individuals often scan their surroundings to gain a preliminary understanding of the environment before executing the action in unfamiliar settings, leading to longer gaze duration for task-relevant objects. As familiarity with the scene increases, the gaze becomes more focused, and the gaze duration correspondingly decreases. This approach ensures the authenticity and naturalness of the gaze data, accurately reflecting real-world gaze behavior.

### 3.2 Data Annotation

**3D Hand Pose.** 12 synchronized ZCAM cameras afford us an exhaustive 3D perspective of the hand, as shown in Figure 2(a). By harnessing the capabilities of MediaPipe [35], we execute 2D hand keypoint tracking across individual video frames. Through the application of triangulation algorithms, we transition the 2D keypoints observed from disparate views to their respective 3D coordinates in global space (shown in Figure 2(b)). Subsequently, we derive the corresponding MANO [42] parameters via an optimization process. To guarantee the physical plausibility and naturalness of the hand poses produced, we integrate pose constraints within the optimization framework. These constraints delineate the permissible range of joint angles, ensuring the hand parameters adhere to realistic anatomical limitations.

**Object 6D Pose.** In our dataset, we exclusively feature rigid objects, enabling us to determine the 6D pose of each object by tracking reflective markers attached to their surfaces via Optitrack. To minimize interference with natural interactions and prevent occlusions that could hinder marker recognition, we strategically placed a minimum of eight 3mm markers on each object. Before

data collection, we employ a 3D scanner to capture the precise geometry of the object surfaces, representing each object with a mesh structure. The Iterative Closest Point(ICP) algorithm is utilized to ascertain the markers’ relative positions on the objects. Consequently, the reflective points detected by OptiTrack are translated into the 6D pose of the object, facilitating accurate and comprehensive pose estimation. Figure 2(d) shows our object repository acquired by scanner and tracking process.

**Gaze Acquisition.** The eye tracker provides highly accurate 2D gaze data from the ego-centric viewpoint, which can then be translated into the direction of 3D gaze. However, due to the inherent limitations of the eye tracker in capturing depth information, the resulting 3D gaze data is subject to significant inaccuracies. To address this issue, we leverage depth cameras to refine and correct the impaired 3D gaze data. The initially acquired 3D gaze information is fraught with noise. Through post-processing, which includes the removal of gaze data with very short annotation durations and the application of smoothing techniques, we manage to extract gaze data rich in intent information. Figure 2(c) shows the gaze during data collection.

### 3.3 Data Statistics

Our dataset encompasses 479 sequences with an average duration of 19.1 seconds and 2-4 objects per sequence, further divisible into 812 subsequences. Among these, 51 sets are dedicated to assembly tasks. We collect 33 different objects within this collection, the smallest of which is a chess piece with a height of 7cm and a mere diameter of 2cm. Each sequence is accompanied by a task-level description, which varies in complexity, and includes repositioning objects to another location, selecting specific targets from cluttered environments, organizing items from disarray into order, and assembling furniture. This rich variety aims to provide comprehensive insights into the intricate dynamics of interactive behaviors.

## 4 Gaze-guided Hand-Object Interaction Synthesis

Gaze behavior acts as a significant indicator of human intention, offering insights into the cognitive mechanisms driving motions. Investigating the role of gaze in hand-object interactions is of significant importance for VR/AR and Human-Robot interaction applications. Therefore, we propose a new task, Gaze-Guided Hand-Object Interaction Synthesis. The specific task definition is outlined in Section 4.1. Figure 3 shows the framework of our method. To generate more realistic and natural hand-object interaction motions, we designed a hierarchical framework centered on GHO-Diffusion. In pre-diffusion, we decoupled gaze conditions into spatial-temporal feature and goal pose conditions across varying levels of information granularity (Section 4.2). Then based on these conditions, we design the GHO-Diffusion to generate object motions consistent with gaze and hand motions from the initial pose to the goal pose (Section 4.3). For post-diffusion, we leverage contact-consistency optimization to refine the generated hand motion (Section 4.4).

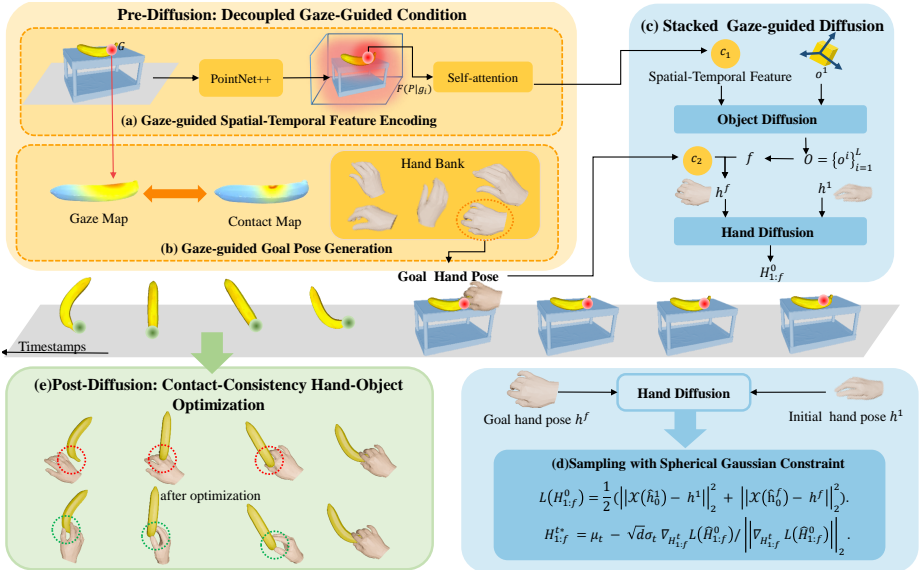


**Fig. 3:** The framework for our method. In the pre-diffusion stage, we decoupled gaze conditions into (a) Gaze-guided Spatial-Temporal Feature Encoding and (b) Gaze-guided Goal Pose Generation. Then based on these conditions, we design (c) GHODiffusion for stacked gaze-guided hand-object motion generation, and in hand diffusion, (d) Spherical Gaussian constraint is introduced for fine-grained guidance. In the post-diffusion stage (e), we optimize the hand motions by leveraging the contact consistency.

#### 4.1 Task Definition

We define a gaze-consistent hand-object interaction sequence with length  $L$  as  $S = \langle G, H, O \rangle$ .  $G = \{g^i\}_{i=1}^L$  is defined as the gaze sequence, where  $g_i \in \mathbb{R}^3$  represents the gaze point in the  $i^{\text{th}}$  frame.  $H = \{h^i\}_{i=1}^L$  is defined as the hand motion sequence, where  $h^i = \{R_h^i, T_h^i, \theta^i\} \in \mathbb{R}^{99}$  follow the MANO [42] parameter representation and the rotations are represented using a 6D notation [64]. Specifically, we define  $h_f$  as the goal hand pose and  $f$  is the goal frame index. The goal pose is defined to ensure that the hand and object are in firm contact, with the object remaining stationary.  $O = \{o^i\}_{i=1}^L$  is defined as the object motion sequence, where  $o^i = \{R_o^i, T_o^i\} \in \mathbb{SE}(3)$  denotes object pose. Furthermore, we denote  $P = \{p^n\}_{n=1}^N \in \mathbb{R}^{N \times 3}$  as the set of object vertices, where  $N$  represents the number of object vertices. Thus, given input  $\mathcal{I} = \{G, h^1, o^1, P\}$ , our objective is to derive a subsequent hand-object interaction sequence that is consistent with the gaze and demonstrates natural and authentic interactions between the hand and the object.

#### 4.2 Pre-Diffusion: Decoupled Gaze-Guided Condition

**Gaze-guided Spatial-Temporal Feature Encoding.** Recent work [2, 23] has shown that humans typically initiate their gaze toward an object before interacting with it. Therefore, we locate a gaze-active object through the spatial



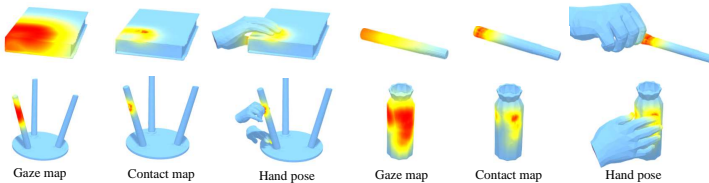


**Fig. 4:** The visualization of gaze map, contact map, and the corresponding hand pose, showing the consistency between gaze and contact.

relationship between gaze and objects. Drawing inspiration from GIMO [63], we design a gaze-guided spatial-temporal feature encoding module for object motion dynamics features. We define  $F_{\text{global}}(P)$  and  $F_{\text{local}}(P)$  as the global and local per-point object spatial feature extracted by PointNet++ [39]. Then according to the spatial relationship between gaze and object points, we can calculate gaze spatial feature  $F(P|g_i)$ ,

$$F(P|g_i) = \frac{1}{d^i} F_{\text{local}}(p_{n^*}), \quad (1)$$

where  $d^i = \min_{n=1}^N \|g^i - p^n\|$  and  $n^* = \arg \min_{n=1}^N \|g^i - p^n\|$ . Subsequently, these spatial features are processed through a self-attention mechanism to extract the final spatial-temporal condition features  $c_1$ .

**Gaze-guided Goal Pose Generation.** Direct synthesis of hand motions conditioned on object motions  $O$  and initial hand poses  $h^1$  presents a considerable challenge, potentially resulting in inconsistent hand-object interactions. To mitigate this issue, we opt to first generate a goal pose, maintaining the contact relationship throughout subsequent hand pose generation. We utilize ContactGen [32] to generate hand poses conditioned on initial object pose and geometry. However, identical conditions may yield different hand poses, which introduces ambiguity into subsequent interactions. We observe that areas receiving more visual attention are more likely to be points of contact. So we define the gaze map as the areas where the gaze is close to object vertices as shown in Figure 4. Therefore, we built a goal pose bank, organizing it with the contact map as keys and corresponding hand poses as values. The contact map  $M = \{m^n\}_{n=1}^N$  is an intermediate result produced by ContactGen. It assigns a contact value  $m^n$  to each of the  $N$  points on the object, quantifying the level of contact at point  $p^n$ . Given a threshold  $\delta$ , if  $d^i < \delta$ , we consider the gaze point  $g^i$  on the point  $p^n$ . For such gaze points, we calculate their gaze-contact consistency value  $V$ , defined as the contact value of the nearest object vertex to gazes  $G$ :

$$V = \frac{1}{|G_\delta|} \sum_{i \in G_\delta} m^{n^*}. \quad (2)$$

Here,  $G_\delta$  is the set of all gaze points satisfying  $d^i < \delta$ , and  $|G_\delta|$  is the number of elements in this set. The hand pose corresponding to the contact map with the highest consistency index is selected as the goal pose  $h^f$ , and then serves as a guide  $c_2$  for synthesizing subsequent hand poses.

### 4.3 GHO-Diffusion: Stacked Gaze-guided Hand-Object Motion Generation

In this section, we propose GHO-Diffusion for stacked gaze-guided hand-object motion generation as shown in Figure 3(c). Leveraging the conditions gaze features  $c_1$  and goal pose  $c_2$  extracting in Section 4.2, we decouple the complex hand-object interaction into two stages, generating object motions and hand motions separately.

**Conditional Diffusion models** Diffusion models [19, 44, 46, 47] are a class of likelihood-based generation models that have gained success in various conditional generation tasks [6, 36, 41, 45, 59]. It contains a fixed forward process  $q(x_t|x_0) = N(\sqrt{\alpha_t}x_0, (1 - \alpha_t)I)$  which gradually adds Gaussian noise to clean data  $x_0$  until it becomes pure noise  $\epsilon \sim \mathcal{N}(0, I)$  and will train a denoiser  $p_\theta(x_t, t, c)$  to gradually denoise  $x_T \sim \mathcal{N}(0, I)$  to generate  $x_0$  in the reverse process. Instead of predicting  $\epsilon_t$  at each time step  $t$ , we follow MDM [50] to predict  $\hat{x}_0$  and optimizing  $p_\theta(x_t, t, c)$  using the simple objective function:

$$L_{\text{simple}} = \mathbb{E}_{x_0 \sim q(x_0|c), t \sim [1, T]} \|x_0 - p_\theta(x_t, t, c)\|_2^2. \quad (3)$$

The reverse process can be formulated as

$$x_{t-1} = \sqrt{\alpha_{t-1}}p_\theta(x_t, t, c) + \sqrt{1 - \alpha_{t-1}}\epsilon. \quad (4)$$

During sampling, we apply classifier-free guidance to get the weighted posterior of  $\hat{x}_0$ :

$$p_\theta(x_t, t, c) = p_\theta(x_t, t, \emptyset) + s \cdot (p_\theta(x_t, t, c) - p_\theta(x_t, t, \emptyset)), \quad (5)$$

where we train  $p_\theta(x_t, t, \emptyset)$  by random setting  $t = \emptyset$ .

**Gaze-guided Object Motion Generation** We adopt the architecture design of conditional denoiser in MDM [50] and gaze spatial-temporal features  $c_1$ , object geometry  $P$  and initial pose  $o^1$  features as well as object geometry and pose features, as conditions to generate object motions  $O$ . For training losses, we use the *simple objective function* in Equation 3 and introduce additional translation and vertice loss for training the object motion diffusion model, the loss details and weights will be explained in supplementary.

$$L_{\text{total}} = \lambda_1 L_{\text{simple}} + \lambda_2 L_{\text{trans}} + \lambda_3 L_{\text{verts}} \quad (6)$$

**Goal-guided Hand Motion Generation** We follow the same architecture to generate natural hand motion  $H_{1:f} = \{h^i\}_{i=1}^f$  transitioning from initial hand pose  $h^1$  to goal hand pose  $h^f$ . The length of the motion sequence  $f$  is determined by object motion generation, spanning from the start frame to the frame at which the object initiates its movement. For training losses, we use the *simple objective function* in Equation 3 to train the hand motion diffusion model.

However, when utilizing  $p_\theta(H_{1:f}^t, t, c_2)$  to generate hand motion given  $c_2$  in the sampling stage, there always exists misalignment between input conditions

$c2 = (h^1, h^f)$  and predicted hand motion  $(\hat{h}^1, \hat{h}^f)$ . To address this issue, we apply the guidance at inference time to strengthen the constraint. Noticed that the guidance signal is sparse (only in the initial frame and end frame), we follow OmniControl [53] to construct the guidance objective function with the global hand pose representation of  $h^1$  and  $h^f$ :

$$L(H_{1:f}^0) = \frac{1}{2}(\|\mathcal{X}(\hat{h}_0^1) - h^1\|_2^2 + \|\mathcal{X}(\hat{h}_0^f) - h^f\|_2^2). \quad (7)$$

Here  $\mathcal{X}(\cdot)$  denotes the local-to-global transformation. Since this local-to-global transformation involves aggregating the local hand poses of each frame, the gradient of  $L(H_{1:f}^0)$  can be backpropagated to all frames, thereby densifying the sparse control signal.

At inference time, the likelihood of  $L(H_{1:f}^0)$  can be used for computing the conditional bias:

$$\nabla_{H_{1:f}^t} \log p(H_{1:f}^t | c2) = \log \nabla_{H_{1:f}^t} p(H_{1:f}^t) + \nabla_{H_{1:f}^t} p(c2 | H_{1:f}^t), \quad (8)$$

where  $\nabla_{H_{1:f}^t} p(H_{1:f}^t)$  can be acquired by the pretrained diffusion prior  $p_\theta(H_{1:f}^t, t, c)$ , leaving the conditional bias  $\nabla_{H_{1:f}^t} p(c | H_{1:f}^t)$  unsolved.

Some current HOI works [10, 24, 27, 37, 53] utilize various methods to compute the conditional bias. Some approaches [10, 37, 53] involve optimizing the posterior mean  $\mu_t$  at time  $t$  using  $\mu_t = \mu_t - \nabla_{\mu_t} L(H_{1:f}^0)$  or  $\mu_t = \mu_t - \nabla_{H_{1:f}^t} L(H_{1:f}^0)$ . However, these methods suffer from inaccuracies as the loss function is defined in a clean data distribution rather than a noisy one. In addition, it is not effective because it is often necessary to iterate  $k$  times in the single denoising process for accurate alignment. Other works [24, 27] optimize  $\hat{H}_{1:f}^0$  by  $\hat{H}_{1:f}^0 = \hat{H}_{1:f}^0 - \nabla_{H_{1:f}^t} L(\hat{H}_{1:f}^0)$ , but the optimizing steps take  $\hat{H}_{1:f}^0$  out of the clean data distribution, resulting in unreal hand motion.

Recently, a conditional diffusion method, Diffusion with Spherical Gaussian [55] named DSG, is dedicated to implementing denoising steps with the Spherical Gaussian constraint for conditional diffusion. DSG offers larger, adaptive step sizes while preserving the original data distribution. However, its effectiveness has mainly been shown in image-generation tasks. Motivated by DSG, we also introduce the Spherical Gaussian constraint to the denoising step of our GHO-Diffusion. Its larger step size characteristics facilitate the better fitting of the goal pose, preventing situations of unrealistic scenarios where the hand ultimately fails to reach the object. Additionally, the Spherical Gaussian constraint ensures that the generated hand motion remains within the clean data distribution, resulting in natural and smooth hand motion generation. The ablation study conducted in Experiment 5.2 further validates the effectiveness of denoising with the Spherical Gaussian constraint.

We utilize closed-form solution  $H_{1:f}^{t*}$  which enforces sampling in gradient descent direction while preserving  $H_{1:f}^{t*}$  within noisy data distribution which resulting in the generated  $H_{1:f}^0$  remaining within the clean data manifold:

$$H_{1:f}^{t*} = \mu_t - \sqrt{d} \sigma_t \nabla_{H_{1:f}^t} L(\hat{H}_{1:f}^0) / \|\nabla_{H_{1:f}^t} L(H_{1:f}^0)\|_2. \quad (9)$$

Here  $\sigma_t$  represents the variance in time step  $t$  and  $d$  represents the data dimensions. To enhance generation diversity, we re-weight the direction of  $H_{1:f}^{t*}$  and the sampling point  $H_{1:f}^t$  like a manner Classifier-free guidance:

$$\mathcal{D} = H_{1:f}^t + w(H_{1:f}^{t*} - H_{1:f}^t), \quad (10)$$

$$H_{1:f}^t = \mu_t + \sqrt{d}\sigma_t \mathcal{D} / \|\mathcal{D}\|, \quad (11)$$

where  $w$  represents the guidance rate that lies in  $[0,1]$  and  $\mathcal{D}$  represents the weighted direction.

#### 4.4 Post-Diffusion: Contact-Consistency Hand-Object Optimization

After initiating contact with the object, the hand grasps and moves the object to a different location. During this process, the hand and object remain relatively stationary with respect to each other, moving at a uniform speed, and maintaining consistent contact points. Hence, utilizing the object motion  $O$  and goal hand pose  $h^f$  derived from section 4.2, we can infer the global translation of the hand motion  $H_{f:L} = \{h^i\}_{i=f}^L$  for this phase.

$$h^i = p_k^i + R_o^i (R_o^f)^{-1} (h^f - p_k^f). \quad (12)$$

Leveraging the consistent nature of fingertip-to-object contact, we employ a Contact Consistency Optimization approach to solve for changes in the object’s global rotation.

$$R_h^i = \arg \min_{R_h^i} (J(R_h^i, T_h^i, \theta^i)_{\text{tip}} - p_{\text{tip}}^i). \quad (13)$$

Here,  $J(R_h^i, T_h^i, \theta^i)_{\text{tip}} \in \mathbb{R}^{5 \times 3}$  represents the computed locations of the fingertips, and  $p_{\text{tip}}^i \in \mathbb{R}^{5 \times 3}$  denotes the points on the object closest to the fingertips.

## 5 Experiments

### 5.1 Data Split and Metrics

We divided 812 sequences into a training set with 682 sequences and a test set comprising 130 sequences. To mitigate the model’s potential overfitting to subject-specific traits, the test set exclusively comprises subjects not represented in the training set. Our evaluation metrics are divided into 2 parts: **First**, from the perspectives of motion consistency with gaze and accuracy, we evaluated errors in hand-object translation and rotation, root-relative Mean Per Joint Position Error (MPJPE), and Mean Per Vertex Position Error (MPVPE) in global space. Additionally, we computed the errors in goal pose(Goal) and final object location(FLoc), along with the proportion of trajectory errors less than 10 cm.; **Second**, from the perspective of stability and realism of the hand-object interaction, we evaluate whether the hand-object interaction motion is reasonable through penetration rate and Contact rate.

## 5.2 Baselines

As the first to propose the task about gaze-guided hand-object interaction, we lack established baselines for comparison. Therefore, we proposed 3 baselines based on MDM [50]. The first is an end-to-end framework, which directly trains the model condition on gaze and initial hand and object pose to synthesize subsequent hand-object interaction. The second is a naive two-stage framework that obtains hand and object motions separately without goal pose generation and optimization. The last is our method that the goal pose generation without gaze-guided. For more details on baseline setup, refer to the supplementary. The quantitative results are shown in Table 2. The ratio of contact and penetration must be considered together. Although MDM exhibits a higher contact ratio, it also has a high penetration ratio, which similarly indicates poor generation results. Since the latter two baselines both utilize the results from our first diffusion, the metrics within the object domain are identical for them. Our results indicate that each module of our design is effective, with more visualizations to be presented in the supplementary.

**Table 2:** Quantitative Comparisons with baselines on GazeHOI. The units for the first four metrics are millimeters, while the last three are expressed as ratios.

	Object		Hand		All		
	MPVPE↓	FLoc↓	MPJPE↓	Goal↓	Traj↓	Pene↓	Contact↑
MDM [50]	248.5	192.9	42.55	176.4	99.82	49.45	83.68
Ours w/o GP	133.1	165.5	39.70	189.1	83.03	10.71	31.12
Ours w/o GM	133.1	165.5	21.59	10.19	41.55	8.56	33.79
Ours	<b>133.1</b>	<b>165.5</b>	<b>17.81</b>	<b>8.28</b>	<b>38.92</b>	<b>8.14</b>	<b>36.81</b>

**Table 3:** Ablation study of gaze encoding. w/o S means directly using self-attention to encode gaze without spatial feature extraction.

Method	MPVPE↓	FLoc↓	Traj%
gaze ray	163.2	242.1	61.05
gaze w/o S	159.6	248.9	58.55
Ours	<b>133.1</b>	<b>165.5</b>	<b>56.58</b>

**Table 4:** Ablation study of different Guided Diffusion Techniques. w/o GM means using the goal pose without gaze-contact consistency detection.

Method	MPJPE↓	Goal↓	Traj%
w/o guide	38.33	53.89	85.38
Classifier-guided [9]	36.92	51.25	82.75
OmniControl [53]	23.07	16.03	28.45
Ours w/o GM	20.37	10.19	31.13
Ours	<b>19.09</b>	<b>8.27</b>	<b>27.90</b>

**Ablation Study** To better understand the contribution of each component in our proposed method, we discuss the impact of different gaze encoding methods and guidance strategies in this section. The quantitative results are summarized in Table 3 and Table 4.

**Gaze Encoding.** We explore the efficiency of extracting information from different representations of 3D gaze data, typically categorized as ray-based and point-based without spatial encoding by PointNet++, the results are in Tab 3.

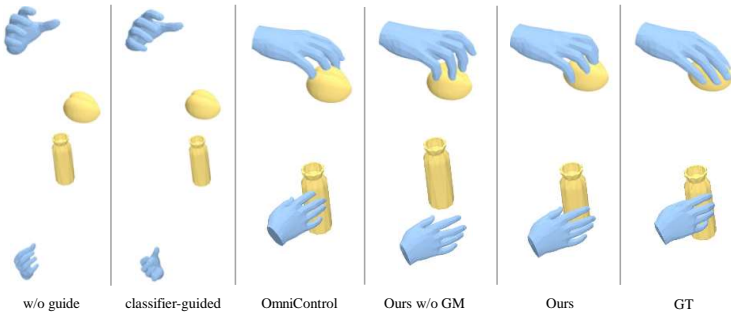


**Fig. 5:** Qualitative results of our goal pose guided that is capable of generating plausible goal poses and achieving them with greater precision. While Omnicontrol [53] can also reach the vicinity of the goal pose, its motion lacks fluidity and naturalness.

Gaze ray is represented as a directional vector. **Goal Guidance Strategies.** We assess the efficacy of different guidance techniques in achieving alignment with the target pose  $h^f$ , with the original diffusion sampling process serving as our baseline. During the denoising steps, we observed an unpredictable rise in the loss function in later stages. Consequently, we implement early stopping after 750 denoising steps. Considering that the guidance method in OmniControl [53] which optimizes the posterior mean at timestep  $t$  forces the alignment by increasing the number of iterations in the last 10 denoising steps, we follow its settings by using the total 1000 denoising steps for enhancing the performance. For standard classifier-guided diffusion, which uses one guidance per denoising step and w/o guidance baseline, we do the same early-stopping strategy for better performance. The result in Table 4 and Figure 5 has demonstrated that the guidance method we adopt is superior to any other baselines. Due to the good nature of the guidance approach we used in preserving the original distribution of generated hand movements, we achieved significantly smaller MPJPE losses as well as trajectory losses. Additionally, as DSG [55] supports a larger range of step sizes, we also gain a better alignment with the goal pose. Please refer to the supplementary for further experimental details and visualization results.

## 6 Conclusion

In summary, this study presents the GazeHOI dataset, the first dedicated resource for examining gaze-guided hand-object interactions, filling a notable void in current research resources. Through the development of the GHO-Diffusion model, this paper introduces an innovative task for synthesizing such interactions within a hierarchy-structured framework. By integrating gaze conditions with the dynamics of hand and object movements, and introducing mechanisms such as the Spherical Gaussian constraint for precise goal pose alignment, our approach significantly advances the field. The extensive experimental validation of both the GazeHOI dataset and our synthesis methodology underscores the potential of gaze guidance in refining the prediction of hand-object motion.

## References

1. Abdelrahman, A.A., Hempel, T., Khalifa, A., Al-Hamadi, A., Dinges, L.: L2cnet: Fine-grained gaze estimation in unconstrained environments. In: 2023 8th International Conference on Frontiers of Signal Processing (ICFSP). pp. 98–102. IEEE (2023)
2. Admoni, H., Scassellati, B.: Social eye gaze in human-robot interaction: a review. *Journal of Human-Robot Interaction* **6**(1), 25–63 (2017)
3. Braun, J., Christen, S., Kocabas, M., Aksan, E., Hilliges, O.: Physically plausible full-body hand-object interaction synthesis. arXiv preprint arXiv:2309.07907 (2023)
4. Chao, Y.W., Yang, W., Xiang, Y., Molchanov, P., Handa, A., Tremblay, J., Narang, Y.S., Van Wyk, K., Iqbal, U., Birchfield, S., Kautz, J., Fox, D.: Dexycb: A benchmark for capturing hand grasping of objects. In: Proceedings of the IEEE/CVF Conference on Computer Vision and Pattern Recognition (CVPR). pp. 9044–9053 (June 2021)
5. Christen, S., Kocabas, M., Aksan, E., Hwangbo, J., Song, J., Hilliges, O.: D-grasp: Physically plausible dynamic grasp synthesis for hand-object interactions. In: Proceedings of the IEEE/CVF Conference on Computer Vision and Pattern Recognition. pp. 20577–20586 (2022)
6. Chung, H., Kim, J., Mccann, M.T., Klasky, M.L., Ye, J.C.: Diffusion posterior sampling for general noisy inverse problems. *International Conference on Learning Representation* (2023)
7. DelPreto, J., Liu, C., Luo, Y., Foshey, M., Li, Y., Torralba, A., Matusik, W., Rus, D.: Actionsense: A multimodal dataset and recording framework for human activities using wearable sensors in a kitchen environment. *Advances in Neural Information Processing Systems* **35**, 13800–13813 (2022)
8. Desanghere, L., Marotta, J.J.: The influence of object shape and center of mass on grasp and gaze. *Frontiers in psychology* **6**, 1537 (2015)
9. Dhariwal, P., Nichol, A.: Diffusion models beat gans on image synthesis. *Advances in neural information processing systems* **34**, 8780–8794 (2021)
10. Diller, C., Dai, A.: Cg-hoi: Contact-guided 3d human-object interaction generation. arXiv preprint arXiv:2311.16097 (2023)
11. Eren Akbiyik, M., Savov, N., Pani Paudel, D., Popovic, N., Vater, C., Hilliges, O., Van Gool, L., Wang, X.: G-memp: Gaze-enhanced multimodal ego-motion prediction in driving. arXiv e-prints pp. arXiv–2312 (2023)
12. Fan, Z., Taheri, O., Tzionas, D., Kocabas, M., Kaufmann, M., Black, M.J., Hilliges, O.: Arctic: A dataset for dexterous bimanual hand-object manipulation. In: Proceedings of the IEEE/CVF Conference on Computer Vision and Pattern Recognition (CVPR). pp. 12943–12954 (June 2023)
13. Fischer, T., Chang, H.J., Demiris, Y.: Rt-gene: Real-time eye gaze estimation in natural environments. In: Proceedings of the European conference on computer vision (ECCV). pp. 334–352 (2018)
14. Ghosh, A., Dabral, R., Golyanik, V., Theobalt, C., Slusallek, P.: Imos: Intent-driven full-body motion synthesis for human-object interactions (2023)
15. Gottlieb, J., Oudeyer, P.Y., Lopes, M., Baranes, A.: Information-seeking, curiosity, and attention: computational and neural mechanisms. *Trends in cognitive sciences* **17**(11), 585–593 (2013)
16. Guan, Y., Chen, Z., Zeng, W., Cao, Z., Xiao, Y.: End-to-end video gaze estimation via capturing head-face-eye spatial-temporal interaction context. *IEEE Signal Processing Letters* **30**, 1687–1691 (2023)

17. Hampali, S., Rad, M., Oberweger, M., Lepetit, V.: Honnotate: A method for 3d annotation of hand and object poses. In: Proceedings of the IEEE/CVF Conference on Computer Vision and Pattern Recognition (CVPR) (June 2020)
18. Hampali, S., Sarkar, S.D., Rad, M., Lepetit, V.: Keypoint transformer: Solving joint identification in challenging hands and object interactions for accurate 3d pose estimation. In: 2022 IEEE/CVF Conference on Computer Vision and Pattern Recognition (CVPR). pp. 11080–11090 (2022). <https://doi.org/10.1109/CVPR52688.2022.01081>
19. Ho, J., Jain, A., Abbeel, P.: Denoising diffusion probabilistic models. *Advances in neural information processing systems* **33**, 6840–6851 (2020)
20. Jiang, H., Liu, S., Wang, J., Wang, X.: Hand-object contact consistency reasoning for human grasps generation. In: Proceedings of the IEEE/CVF International Conference on Computer Vision. pp. 11107–11116 (2021)
21. Karunratanakul, K., Preechakul, K., Suwajanakorn, S., Tang, S.: Guided motion diffusion for controllable human motion synthesis. In: Proceedings of the IEEE/CVF International Conference on Computer Vision. pp. 2151–2162 (2023)
22. Kothari, R., De Mello, S., Iqbal, U., Byeon, W., Park, S., Kautz, J.: Weakly-supervised physically unconstrained gaze estimation. In: Proceedings of the IEEE/CVF Conference on Computer Vision and Pattern Recognition. pp. 9980–9989 (2021)
23. Kratzer, P., Bihlmaier, S., Midlagajni, N.B., Prakash, R., Toussaint, M., Mainprice, J.: Mogaze: A dataset of full-body motions that includes workspace geometry and eye-gaze. *IEEE Robotics and Automation Letters* **6**(2), 367–373 (2020)
24. Kulkarni, N., Rempe, D., Genova, K., Kundu, A., Johnson, J., Fouhey, D., Guibas, L.: Nifty: Neural object interaction fields for guided human motion synthesis. arXiv preprint arXiv:2307.07511 (2023)
25. Kwon, T., Tekin, B., Stühmer, J., Bogo, F., Pollefeys, M.: H2o: Two hands manipulating objects for first person interaction recognition. In: Proceedings of the IEEE/CVF International Conference on Computer Vision (ICCV). pp. 10138–10148 (October 2021)
26. Li, H., Lin, X., Zhou, Y., Li, X., Huo, Y., Chen, J., Ye, Q.: Contact2grasp: 3d grasp synthesis via hand-object contact constraint. arXiv preprint arXiv:2210.09245 (2022)
27. Li, J., Clegg, A., Mottaghi, R., Wu, J., Puig, X., Liu, C.K.: Controllable human-object interaction synthesis. arXiv preprint arXiv:2312.03913 (2023)
28. Li, Q., Wang, J., Loy, C.C., Dai, B.: Task-oriented human-object interactions generation with implicit neural representations. arXiv preprint arXiv:2303.13129 (2023)
29. Liang, H., Bao, J., Zhang, R., Ren, S., Xu, Y., Yang, S., Chen, X., Yu, J., Xu, L.: Omg: Towards open-vocabulary motion generation via mixture of controllers. arXiv preprint arXiv:2312.08985 (2023)
30. Lin, P., Xu, S., Yang, H., Liu, Y., Chen, X., Wang, J., Yu, J., Xu, L.: Handdif-fuse: Generative controllers for two-hand interactions via diffusion models. arXiv preprint arXiv:2312.04867 (2023)
31. Liu, M., Tang, S., Li, Y., Rehg, J.M.: Forecasting human-object interaction: joint prediction of motor attention and actions in first person video. In: Computer Vision–ECCV 2020: 16th European Conference, Glasgow, UK, August 23–28, 2020, Proceedings, Part I 16. pp. 704–721. Springer (2020)
32. Liu, S., Zhou, Y., Yang, J., Gupta, S., Wang, S.: Contactgen: Generative contact modeling for grasp generation. In: Proceedings of the IEEE/CVF International Conference on Computer Vision. pp. 20609–20620 (2023)



33. Liu, Y., Yang, H., Si, X., Liu, L., Li, Z., Zhang, Y., Liu, Y., Yi, L.: Taco: Benchmarking generalizable bimanual tool-action-object understanding. arXiv preprint arXiv:2401.08399 (2024)
34. Liu, Y., Liu, Y., Jiang, C., Lyu, K., Wan, W., Shen, H., Liang, B., Fu, Z., Wang, H., Yi, L.: Hoi4d: A 4d egocentric dataset for category-level human-object interaction. In: Proceedings of the IEEE/CVF Conference on Computer Vision and Pattern Recognition (CVPR). pp. 21013–21022 (June 2022)
35. Lugaresi, C., Tang, J., Nash, H., McClanahan, C., Uboweja, E., Hays, M., Zhang, F., Chang, C., Yong, M.G., Lee, J., Chang, W., Hua, W., Georg, M., Grundmann, M.: Mediapipe: A framework for building perception pipelines. CoRR **abs/1906.08172** (2019), <http://arxiv.org/abs/1906.08172>
36. Meng, C., He, Y., Song, Y., Song, J., Wu, J., Zhu, J.Y., Ermon, S.: Sdedit: Guided image synthesis and editing with stochastic differential equations. arXiv preprint arXiv:2108.01073 (2021)
37. Peng, X., Xie, Y., Wu, Z., Jampani, V., Sun, D., Jiang, H.: Hoi-diff: Text-driven synthesis of 3d human-object interactions using diffusion models. arXiv preprint arXiv:2312.06553 (2023)
38. Pi, H., Peng, S., Yang, M., Zhou, X., Bao, H.: Hierarchical generation of human-object interactions with diffusion probabilistic models. In: Proceedings of the IEEE/CVF International Conference on Computer Vision. pp. 15061–15073 (2023)
39. Qi, C.R., Yi, L., Su, H., Guibas, L.J.: Pointnet++: Deep hierarchical feature learning on point sets in a metric space. *Advances in neural information processing systems* **30** (2017)
40. Ragusa, F., Furnari, A., Livatino, S., Farinella, G.M.: The meccano dataset: Understanding human-object interactions from egocentric videos in an industrial-like domain. In: Proceedings of the IEEE/CVF Winter Conference on Applications of Computer Vision. pp. 1569–1578 (2021)
41. Rombach, R., Blattmann, A., Lorenz, D., Esser, P., Ommer, B.: High-resolution image synthesis with latent diffusion models. In: Proceedings of the IEEE/CVF conference on computer vision and pattern recognition. pp. 10684–10695 (2022)
42. Romero, J., Tzionas, D., Black, M.J.: Embodied hands: Modeling and capturing hands and bodies together. *ACM Transactions on Graphics, (Proc. SIGGRAPH Asia)* **36**(6) (Nov 2017)
43. Schneider, W.X.: Vam: A neuro-cognitive model for visual attention control of segmentation, object recognition, and space-based motor action. *Visual Cognition* **2**(2-3), 331–376 (1995). <https://doi.org/10.1080/13506289508401737>, <https://doi.org/10.1080/13506289508401737>
44. Sohl-Dickstein, J., Weiss, E., Maheswaranathan, N., Ganguli, S.: Deep unsupervised learning using nonequilibrium thermodynamics. In: International conference on machine learning. pp. 2256–2265. PMLR (2015)
45. Song, J., Meng, C., Ermon, S.: Denoising diffusion implicit models. arXiv preprint arXiv:2010.02502 (2020)
46. Song, Y., Ermon, S.: Generative modeling by estimating gradients of the data distribution. *Advances in neural information processing systems* **32** (2019)
47. Song, Y., Sohl-Dickstein, J., Kingma, D.P., Kumar, A., Ermon, S., Poole, B.: Score-based generative modeling through stochastic differential equations. arXiv preprint arXiv:2011.13456 (2020)
48. Taheri, O., Choutas, V., Black, M.J., Tzionas, D.: Goal: Generating 4d whole-body motion for hand-object grasping. In: Proceedings of the IEEE/CVF Conference on Computer Vision and Pattern Recognition. pp. 13263–13273 (2022)

49. Tanaka, M., Fujiwara, K.: Role-aware interaction generation from textual description. In: Proceedings of the IEEE/CVF International Conference on Computer Vision. pp. 15999–16009 (2023)
50. Tevet, G., Raab, S., Gordon, B., Shafir, Y., Cohen-Or, D., Bermano, A.H.: Human motion diffusion model. arXiv preprint arXiv:2209.14916 (2022)
51. Wu, Q., Shi, Y., Huang, X., Yu, J., Xu, L., Wang, J.: Thor: Text to human-object interaction diffusion via relation intervention. arXiv preprint arXiv:2403.11208 (2024)
52. Wu, Y., Wang, J., Zhang, Y., Zhang, S., Hilliges, O., Yu, F., Tang, S.: Saga: Stochastic whole-body grasping with contact. In: European Conference on Computer Vision. pp. 257–274. Springer (2022)
53. Xie, Y., Jampani, V., Zhong, L., Sun, D., Jiang, H.: Omnicontrol: Control any joint at any time for human motion generation. arXiv preprint arXiv:2310.08580 (2023)
54. Xu, S., Li, Z., Wang, Y.X., Gui, L.Y.: Interdiff: Generating 3d human-object interactions with physics-informed diffusion. In: Proceedings of the IEEE/CVF International Conference on Computer Vision. pp. 14928–14940 (2023)
55. Yang, L., Ding, S., Cai, Y., Yu, J., Wang, J., Shi, Y.: Guidance with spherical gaussian constraint for conditional diffusion. arXiv preprint arXiv:2402.03201 (2024)
56. Yang, L., Li, K., Zhan, X., Wu, F., Xu, A., Liu, L., Lu, C.: Oakink: A large-scale knowledge repository for understanding hand-object interaction. In: Proceedings of the IEEE/CVF Conference on Computer Vision and Pattern Recognition (CVPR). pp. 20953–20962 (June 2022)
57. Zhang, H., Ye, Y., Shiratori, T., Komura, T.: Manipnet: neural manipulation synthesis with a hand-object spatial representation. ACM Transactions on Graphics (ToG) **40**(4), 1–14 (2021)
58. Zhang, J., Luo, H., Yang, H., Xu, X., Wu, Q., Shi, Y., Yu, J., Xu, L., Wang, J.: Neuraldome: A neural modeling pipeline on multi-view human-object interactions. In: Proceedings of the IEEE/CVF Conference on Computer Vision and Pattern Recognition (CVPR). pp. 8834–8845 (June 2023)
59. Zhang, L., Rao, A., Agrawala, M.: Adding conditional control to text-to-image diffusion models. In: Proceedings of the IEEE/CVF International Conference on Computer Vision. pp. 3836–3847 (2023)
60. Zhang, W., Huang, M., Zhou, Y., Zhang, J., Yu, J., Wang, J., Xu, L.: Both2hands: Inferring 3d hands from both text prompts and body dynamics. arXiv preprint arXiv:2312.07937 (2023)
61. Zhao, C., Zhang, J., Du, J., Shan, Z., Wang, J., Yu, J., Wang, J., Xu, L.: I’m hoi: Inertia-aware monocular capture of 3d human-object interactions. arXiv preprint arXiv:2312.08869 (2023)
62. Zheng, J., Zheng, Q., Fang, L., Liu, Y., Yi, L.: Cams: Canonicalized manipulation spaces for category-level functional hand-object manipulation synthesis. In: Proceedings of the IEEE/CVF Conference on Computer Vision and Pattern Recognition. pp. 585–594 (2023)
63. Zheng, Y., Yang, Y., Mo, K., Li, J., Yu, T., Liu, Y., Liu, C.K., Guibas, L.J.: Gimo: Gaze-informed human motion prediction in context. In: European Conference on Computer Vision. pp. 676–694. Springer (2022)
64. Zhou, Y., Barnes, C., Lu, J., Yang, J., Li, H.: On the continuity of rotation representations in neural networks. In: Proceedings of the IEEE/CVF Conference on Computer Vision and Pattern Recognition. pp. 5745–5753 (2019)